Journal of Hazardous Materials 189 (2011) 586–594

Contents lists available at ScienceDirect

Journal of Hazardous Materials

journal homepage: www.elsevier.com/locate/jhazmat

Enhanced removal of triphosphate by MgCaFe-Cl-LDH: Synergism of precipitation with intercalation and surface uptake

Jizhi Zhou[a], Zhi Ping Xu[b,*], Shizhang Qiao[b], Qiang Liu[a], Yunfeng Xu[a], Guangren Qian[a,**]

[a] School of Environmental and Chemical Engineering, Shanghai University, No. 333 Nanchen Rd., Shanghai 200444, PR China
[b] ARC Centre of Excellence for Functional Nanomaterials, Australian Institute of Bioengineering and Nanotechnology, The University of Queensland, Brisbane, QLD 4072, Australia

ARTICLE INFO

Article history:
Received 6 October 2010
Received in revised form 23 February 2011
Accepted 23 February 2011
Available online 2 March 2011

Keywords:
Triphosphate
Layered double hydroxide (LDH)
Intercalation
Dissolution
Precipitation

ABSTRACT

Triphosphate (TPP) is an important form of phosphate pollutants while its removal investigation has been just started now. This research examined the removal of triphosphate using $Mg_{2-x}Ca_xFeCl$-LDH (x = 0–2) as absorbents. We found that the removal of triphosphate over Mg_2FeCl-LDH mainly underwent the surface adsorption and the near-edge intercalation, with the practical removal amount (9–11 mg(P)/g) corresponding to 10–15% of the theoretical one. In contrast, Ca_2FeCl-LDH removed a higher amount of triphosphate (56.4 mg(P)/g). The comprehensive analysis of the triphosphate-uptake products with XRD/XPS/FTIR reveals that Ca_2FeCl-LDH dissolves first and then released Ca^{2+} ions react with triphosphate (TPP) to form insoluble Ca-TPP precipitate. Combination of these two different removal mechanisms enables $Mg_{0.5}Ca_{1.5}FeCl$-LDH to take up 84.2 mg(P)/g from aqueous solution under similar conditions.

1. Introduction

In recent decades, layered double hydroxides (LDHs), known as anionic clays or hydrotalcite-like compounds (HTlcs), have been intensively investigated due to their wide applications in many fields, such as gene/drug delivery, catalysis, and anion removal and separation [1,2]. Structurally, LDH is composed of positively charged brucite-like sheets with intercalated anions in the hydrated interlayer regions to balance the positive charges. A typical composition can be represented as the following general formula: $[M^{2+}{}_{1-x}M^{3+}{}_x(OH)_2]^{x+}[(A^{n-})^{x/n}\cdot yH_2O]^{x-}$, where M^{2+} represents any divalent cations (Mg^{2+}, Zn^{2+}, Co^{2+}, Ni^{2+}, Cu^{2+} and/or Ca^{2+}), M^{3+} any trivalent cations (Al^{3+}, Cr^{3+}, and/or Fe^{3+}) and A^{n-} any interlayer anions (Cl^-, $NO_3{}^-$, $SO_4{}^{2-}$, $CO_3{}^{2-}$ and many others). In particular, due to the relatively weak interlayer bonding, anions such as Cl^- and $NO_3{}^-$ intercalated in LDHs are readily exchanged with various organic and inorganic anions [1].

By virtue of the anion exchange capacity, LDHs have great potential to take up and remove anionic contaminants from polluted waters. For example, a number of inorganic (such as phosphates, arsenate, selenate, and chromate) [3–5] and organic anions (folate, nitrophenol, terephthalate, etc.) [6–8] can be removed using LDH-based materials. Note that phosphorus-relevant anions (phosphate, diphosphate and polyphosphate, etc.) are nutrient for many aqueous plants, causing a fast growth of aquatic vegetation and leading to severe aquatic ecosystem destroy. Therefore their removal from aqueous solution attracts much attention, in which LDH-based materials are actively examined [5,9]. In particular, triphosphate ($P_3O_{10}{}^{5-}$ TPP) is an important species of phosphate that mainly comes from used detergents and causes the growth of aquatic plants and cyanobacteria because TPP is slowly degraded to orthophosphate [10] and has a long life time. Thus, TPP removal is necessary from the wastewaters.

Hydrolysis of TPP itself and immobilization by minerals are the possible TPP removal options [11–13]. As a TPP adsorbent, LDH shows some potential to effectively take up TPP due to its anion exchange capacity. For example, the removal of triphosphate (TPP) using Mg-Al-LDH was reported, in which about 43 mg (TPP)/g, i.e. 16 mg(P)/g, was taken up at 25 °C [9], where anion exchange is the main process for TPP removal. In recent research, our laboratory used CaAlCl-LDH and took the advantage of the Ca-hydroxide soluble property to effectively remove phosphate by forming hydroxyapatite [5]. Seida and Nakano also found that the dissolution of CaFe-LDH is responsible for the excess removal amount of orthophosphate [14], largely due to the formation of Ca-phosphate precipitate. To our knowledge, there is seemingly no report regarding the removal of TPP over CaFe-LDH until now.

Herein, the objectives of this research were to (1) investigate the removal behaviors of TPP over Mg_2Fe-Cl-LDH and Ca_2Fe-Cl-LDH; (2) analyze the precipitation products in structure and composition; (3) identify the TPP removal mechanisms over these two LDHs.

* Corresponding author. Tel.: +61 7 33463809; fax: +61 7 33463973.
** Corresponding author. Tel.: +86 21 66137758.
E-mail addresses: gordonxu@uq.edu.au (Z.P. Xu), grqian@shu.edu.cn (G. Qian).

0304-3894/$ – see front matter © 2011 Elsevier B.V. All rights reserved.
doi:10.1016/j.jhazmat.2011.02.078

Our results showed that TPP was just adsorbed on the surface and intercalated into near-edge interlayer of MgFeCl-LDH, while the removal of TPP over CaFeCl-LDH was attributed to the formation of Ca-TPP precipitates; and (4) demonstrate whether there is a synergic effect between these removal processes.

2. Experimental

2.1. Preparation of LDH

The Fe(III)-based LDHs (e.g. $Mg_{2-x}Ca_xFeCl$-LDH, $x = 0–2$) were prepared with a coprecipitation method. Typically, to make Ca_2FeCl-LDH, 7.350 g $CaCl_2{\cdot}2H_2O$ (0.05 mol) and 6.762 g $FeCl_3{\cdot}10H_2O$ (0.02 mol) were dissolved in 50 ml water (solution A). Solution B was prepared by dissolving 4.80 g NaOH (0.12 mol) in 100 ml water. Ca_2FeCl-LDH was precipitated by pouring solution A into solution B under vigorous stirring. The suspension was aged with magnetic stirring for 18 h at 25 °C. Solid precipitate was obtained by centrifuged at 4500 rpm for 10 min and washed twice with 150 ml water each time. To minimize the contamination of carbon dioxide, deionized water was used in the whole process and precipitation/aging was run in N_2 atmosphere. After drying at 50 °C, the powder sample was collected for characterization and removal test. Mg_2FeCl-LDH was prepared in the same way by replacing $CaCl_2$ with $MgCl_2$.

In addition, a few MgCaFeCl-LDHs were synthesized in the similar way. The nominal formula were $Mg_{0.5}Ca_{1.5}FeCl$-LDH, $Mg_{1.0}Ca_{1.0}FeCl$-LDH, and $Mg_{1.5}Ca_{0.5}FeCl$-LDH, corresponding to the molar ratio of Mg/Ca = 1:3, 1:1 and 3:1 while the molar ration of [Ca + Mg]/Fe was kept at 2:1.

2.2. Removal of TPP

TPP solutions with various concentrations of P were prepared by dissolving $Na_5P_3O_{10}$ in deionized water. All experiments were conducted at 25 °C and initial pH of 8.0 in a water-batch with 200 rpm shaking. The isotherm experiment was carried out by adding 0.020 g of LDH in 100 ml solution with the initial concentration of element P in phosphate from 0 to 45 mg/L. Uptake was continued for 24 h under shaking. The removal kinetics of TPP over LDHs was examined by monitoring the P concentration over LDH (0.40 g) in 2000 ml solution with [P] = 45 mg/L. At the selected time, 5 ml solution was withdrawn to determine P concentration left in solution. Prior to the [P] determination, the withdrawn liquid was filtered through 0.22 μm micropore filter membrane to remove any solid particles. The TPP-uptake LDHs were denoted as P-$Mg_{2-x}Ca_xFeCl$-LDH. HCa_2FeCl-LDH and HMg_2FeCl-LDH meant hydrolyzed Ca_2FeCl-LDH and Mg_2FeCl-LDH in phosphate free solution. In addition, P-HCa_2FeCl-LDH represented TPP-uptake HCa_2FeCl-LDH. The solid sample was washed with distilled water and dried at 60 °C in vacuum oven.

The effect of ionic strength was examined in 0.1 M NaCl solution under the same conditions. Moreover, the reversibility of P-uptake products was examined by placing 0.020 g P-Ca_2FeCl-LDH and P-Mg_2FeCl-LDH in 100 ml P-free water (pH = 8.0) after 24 h shaking at 25 °C.

2.3. Characterization

All pH values were measured with a portable pH meter with a glass electrode (Aqua Cond/pH, TPS). The P concentration was determined by a UV-2450 spectrophotometer (SHIMAZDU) at 700 nm following the molybdenum blue method after digested by 5% (w/w) potassium persulfate [15]. Thus, the adsorption amount of TPP on LDH was calculated according to the difference between the initial P concentration and that at the tested point.

Inductively Coupled Plasma-Atom Emission Spectrum (ICP-AES, Prodigy, Leeman Co.) was employed to determine the metal contents in LDHs. The dried solid sample (0.020 g) was dissolved in 40 ml 1:1(v/v) HCl solution. The resultant acid solution was diluted in 100 ml with deionized water and filtered with 0.22 μm micropore membrane before ICP test.

XRD measurements were performed on Miniflex X-ray diffractometer (Rigaku) using Co Kα radiation (λ = 0.1789 nm) at 40 kV, at a scanning rate of 2° min^{-1}. Powder data file (ICDD-JCPDS) was utilized for analysis of the patterns. ATR-FTIR spectra were recorded on Nicolet 6700 (Thermo Ltd.) with the scanning range from 400 to 1800 cm^{-1}. The surface area of the samples was measured by N_2 sorption at liquid nitrogen temperature in a Quantachrome Quantasorb SI Analyser using Brunner–Emmett–Teller (BET) equation to estimate the surface area at a relative pressure of $P/P_o = 0.05–0.30$.

XPS spectra were acquired using a Kratos Axis ULTRA X-ray Photoelectron Spectrometer incorporating a 165 mm hemispherical electron energy analyzer. The incident radiation was monochromatic Al Kα X-rays (1486.6 eV) at 150 W (15 kV, 10 mA). Survey scans were carried out over 1200–0 eV binding energy (BE) range at a step of 1.0 eV and a dwell time of 100 ms. High-resolution scans were run at a step of 0.05 eV and a dwell time of 250 ms. The BE of each element was calibrated with the binding energy of C 1s core level at 284.6 eV. The dried P-uptake sample was directly used for XPS analysis.

The morphology of P-uptake Ca_2Fe-Cl-LDH and Mg_2Fe-Cl-LDH was analyzed by transmission electron microscope (TEM, FEI Tecnai 20) equipped with an energy dispersive X-ray spectroscopy (EDXs) analysis unit (AMETEK). The sample was ultrasonically dispersed in ethanol, dropped on the copper grid and dried in the air.

3. Results and discussion

3.1. Characteristic of LDH samples

The LDH phase of as-synthesized samples has been identified with XRD patterns, as shown in Fig. 1. For example, Mg_2FeCl-LDH exhibits its characteristic diffractions, such as peaks (0 0 3), (0 0 6), (0 1 2) and (1 1 0)/(1 1 3), with a *d*-spacing of 0.803 nm (Table 1). The observed lattice parameters (*a* and *c*) are similar to the reported elsewhere [16]. As also shown in Table 1, the determined Mg/Fe molar ratio is 1.92, indicating Mg_2FeCl-LDH has a chemical formula similar to expected $Mg_2Fe(OH)_6Cl{\cdot}2H_2O$ (MW: 278). As shown in Fig. 1(b), the XRD pattern also identifies that Ca_2FeCl-LDH is of LDH phase (PDF 31-0245), with a *d*-spacing of 0.788 nm. Ca_2FeCl-LDH has lattice parameter *a* of 0.589 nm (Table 1) due to Ca^{2+} seven-coordination structure [17]. The measured Ca/Fe molar ratio (1.91) also means that the chemical formula is approximately $Ca_2Fe(OH)_6Cl{\cdot}2H_2O$ (MW: 309). FTIR spectra (Fig. 2) indicate that both Mg_2Fe-Cl-LDH and Ca_2Fe-Cl-LDH have similar vibrations characteristic of the LDH structure, including the band of HOH bending in water molecule at 1550–1700 cm^{-1}, the vibrations of metal-O (or metal-OH) bond at 500–750 cm^{-1} and the vibration of M–O–M lattice at 428–433 cm^{-1} [18]. In addition, two raw LDHs were slightly CO_2-contaminated as the corresponding CO_3^{2-} peak at 1350–1450 cm^{-1} was relatively weak [19].

The very interesting issue is the stability of LDHs in water. After 0.20 g of Mg_2FeCl-LDH was shaken in 1 L of deionized water for 24 h, the collected solid (HMg_2FeCl-LDH) exhibited an XRD pattern similar to its pristine LDH (Fig. 1(a)), with a *d*-spacing of 0.795 nm (Table 1). The crystallite thickness in plane (0 0 3) is also similar to that of Mg_2FeCl-LDH (Table 1). In sharp contrast, the hydrolyzed Ca_2FeCl-LDH lost its original LDH structure, becoming an amorphous material with minimum $CaCO_3$ in the collected solid (Fig. 1(b)). Moreover, FTIR spectra confirm the consistent structure

Table 1
Chemical composition, textural properties and lattice parameters of LDHs before and after P removed and hydrated products.

Sample	*d*-Spacing[a] (nm)	*a*[b] (nm)	*c*[b] (nm)	Thickness[c] (nm)	M(II)/Fe[d] molar ratio	Specific surface area (m^2/g)
Mg_2FeCl-LDH	0.803	0.311	2.41	19.1	1.92	67
HMg_2FeCl-LDH	0.795	0.311	2.38	20.2	1.60	100
P-Mg_2FeCl-LDH	0.798	0.311	2.39	14.7	1.45	91
Ca_2FeCl-LDH	0.788	0.589	2.36	23.0	1.91	16
HCa_2FeCl-LDH	n/a[e]	n/a	n/a	n/a	0.24	219
P-Ca_2FeCl-LDH	n/a	n/a	n/a	n/a	1.04	83

[a] *d*-Spacing is calculated via equation: d-spacing = $(d_{003} + 2d_{006})/2$.
[b] Lattice parameters a and c are given by the estimation: $a = 2d_{110}$ and $c = 3d$-spacing, respectively.
[c] The average value calculated from FWHM of peak (0 0 3) and (0 0 6) using the Scherrer equation.
[d] Determined by ICP.
[e] n/a denotes "data not available".

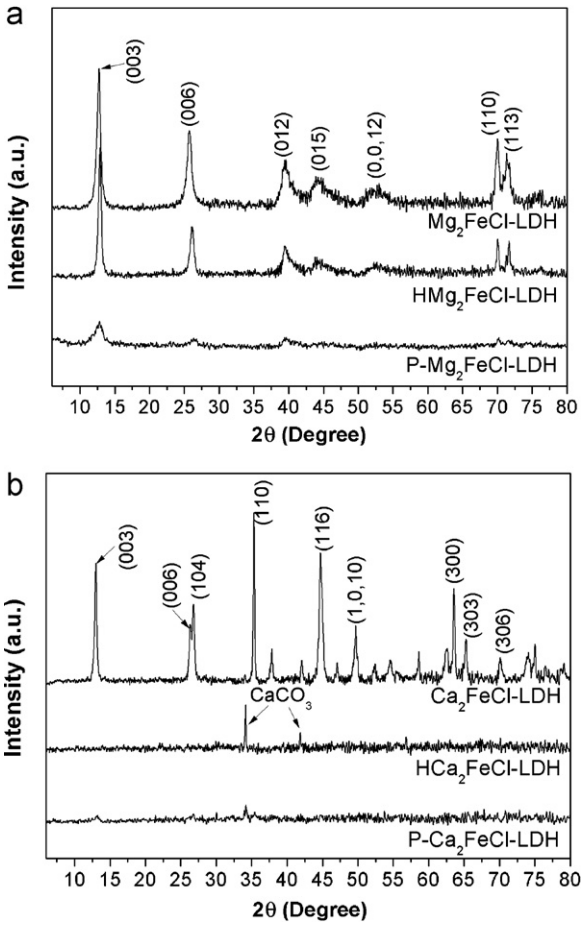

Fig. 1. XRD patterns of Mg_2FeCl-LDH and Ca_2FeCl-LDH before and after TPP removal and their hydrolyzed products.

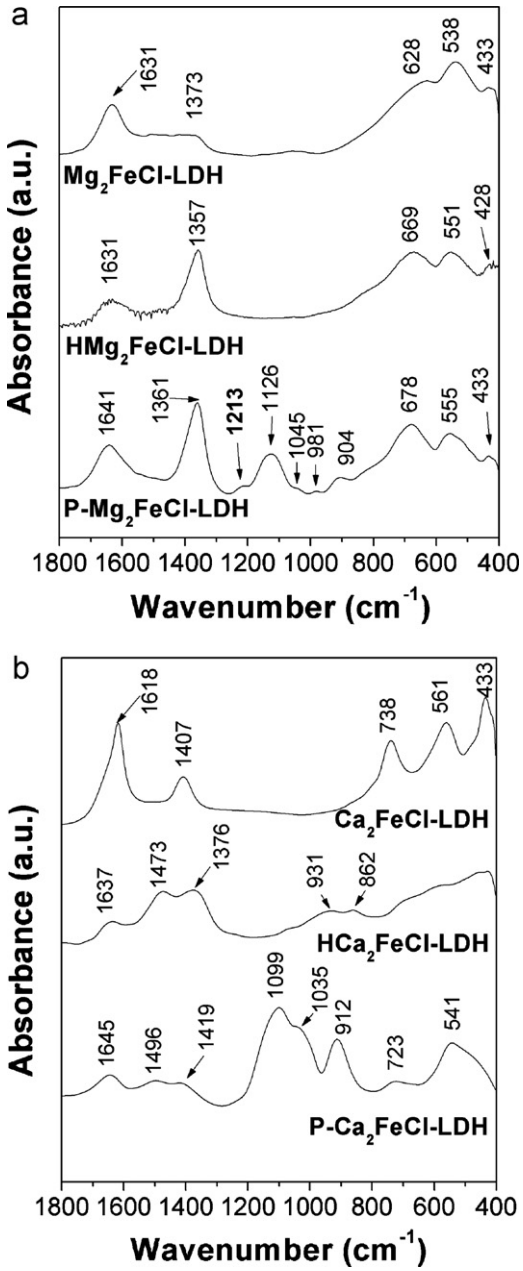

Fig. 2. FTIR spectra of adsorbents before and after TPP removal, and their hydrolyzed products.

of Mg_2Fe-Cl-LDH and HMg_2Fe-Cl-LDH by the same vibration peaks, except for the different intensity (Fig. 2(a)). The absence of IR vibrations of M–O–M lattice and M–O bending demonstrate the loss of the LDH structure in HCa_2FeCl-LDH. In addition, the vibration of $CaCO_3$ in HCa_2FeCl-LDH was revealed by the splitting of CO_3 ($\nu 1$) in calcite into 1473 and 1376 cm^{-1} (Fig. 2(b)) [20].

Furthermore, the element analysis reveals that the Mg/Fe molar ratio in HMg_2FeCl-LDH was reduced to 1.60, while the Ca/Fe molar ratio only to 0.24 (Table 1), both indicating that Mg and Ca are leached out, but much more severely in the latter case. If only the individual hydroxide is concerned, $Ca(OH)_2$ ($Ksp = 5.02 \times 10^{-6}$ [21]) is much more soluble than $Mg(OH)_2$ ($Ksp = 5.61 \times 10^{-12}$ [21]), and $Fe(OH)_3$ is almost insoluble at pH = 8–11 ($Ksp = 2.79 \times 10^{-39}$ [21]). The dissolution properties of these three hydroxides are mostly inherited in the corresponding LDHs, which leads most Ca to dis-

Table 2
Final pHs and saturation triphosphate uptake amounts of different LDHs at 45 mg/L of initial [P] and initial pH of 8 after 24 h removal.

Sample	Final pH	Adsorption amount	
		(mg/g)	(mg/m^2)
Mg_2FeCl-LDH	9.5	10.5	0.157
Ca_2FeCl-LDH	10.5	56.4	3.53
HMg_2FeCl-LDH	9.4[a]	–	–
HCa_2FeCl-LDH	11.2[a]	7.0[b]	0.032
$Mg_{1.5}Ca_{0.5}FeCl$-LDH	10.1	10.7	–
$Mg_{1.0}Ca_{1.0}FeCl$-LDH	9.8	21.2	–
$Mg_{0.5}Ca_{1.5}FeCl$-LDH	9.3	84.2	–

[a] The pH after hydrolysis of Ca_2Fe-Cl-LDH in the P free solution.
[b] The adsorbed amount was at initial [P] = 25 ppm.

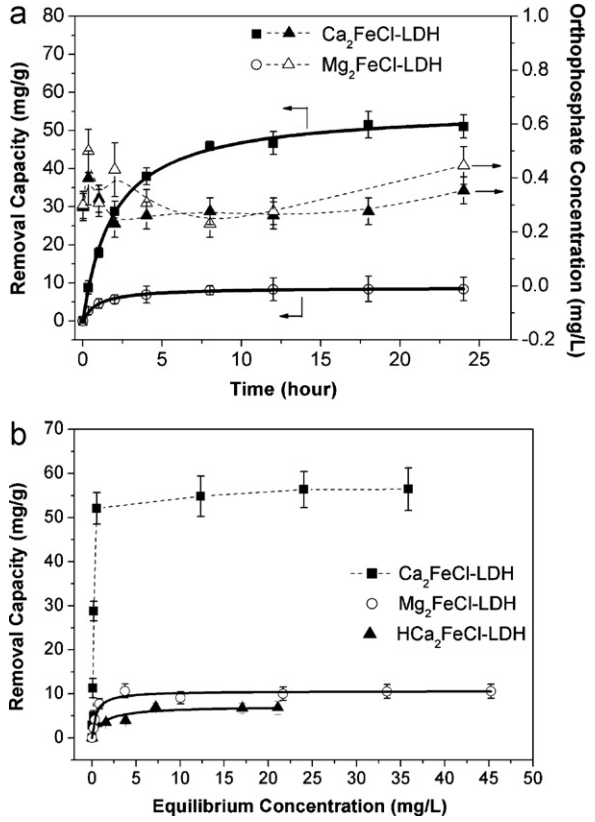

Fig. 3. Removal processes of TPP on LDHs and the hydrolyzed product. (a) Kinetics with orthophosphate concentration. Solid lines are fitting curves from the pseudo-second-order model; dash line refers to the orthophosphate concentration as the function of time; (b) isotherm. Solid and dash lines refer to the removal trend on substrates.

solve in water and gives a higher pH (11.2) while only part of Mg leaches out with a lower pH (9.4) (Table 2) [5]. The leaching of Mg or Ca leaves a Fe-rich network that has a higher surface area (Table 1), which is particularly obvious for HCa_2FeCl-LDH with the specific surface area up to 219 m^2/g. The solubility difference may largely affect the removal behaviors of TPP over these two LDHs, as demonstrated below.

3.2. Removal of TPP on LDHs

The removal process as the function of time is shown in Fig. 3(a). The TPP removal amount (in terms of element P in TPP) over both LDHs was increased with the time. However, Mg_2Fe-Cl-LDH reached removal saturation within 8 h while the saturation time was 18–24 h over Ca_2FeCl-LDH. The saturation amount of TPP over Ca_2FeCl-LDH was nearly 50 mg/g, much higher than that over

Table 3
Fitting parameters for the removal of TPP by LDHs.

Samples	Parameters		
	K_2 (g/mg/h)	Q_2 (mg/g)	R^2
Pseudo-second-order model			
Ca_2FeCl-LDH	9.27×10^{-3}	55.8	0.998
Mg_2FeCl-LDH	0.121	8.74	0.995

Mg_2FeCl-LDH (about 9 mg/g), and the reported over MgAl-LDH (16 mg/g) [4]. The kinetics was well fitted with the pseudo-second-order model (Table 3) [22]. The simulated saturation amount of TPP (Q_2) over Ca_2FeCl-LDH was 6 times as that over Mg_2FeCl-LDH. This difference suggests that the removal process of TPP over these two LDHs follows different removal mechanisms, depending on properties of LDH materials, as discussed in Section 3.4. As the saturation removal was achieved in both cases within 24 h, the isotherm experiment of TPP was thus performed for 24 h.

Fig. 3(b) shows the isotherm experiment of TPP over these two LDHs and hydrolyzed Ca_2FeCl-LDH (e.g. HCa_2FeCl-LDH). Both of Mg_2FeCl-LDH and Ca_2FeCl-LDH show an increasing TPP removal amount with the equilibrium concentration. The maximum TPP removal amount was 10.5 mg/g over by Mg_2FeCl-LDH, and 56.4 mg/g by Ca_2FeCl-LDH. It is well known that the capture of phosphates over MgFe-LDH is actually an anion exchange process [23]. If all Cl ions in Mg_2Fe-Cl-LDH are exchanged with TPP, then the theoretical adsorption amount will be 67 mg(P)/g (assuming 0.72 mmol of TPP substitutes 3.6 mmol of Cl anions in 1 g of Mg_2FeCl-LDH), 6 times higher than that observed in this research. The big gap is presumably attributed to the bigger size of TPP than Cl^-, which makes the diffusion of TPP into the interlayer much more difficult during the exchange process. In fact, after TPP adsorption, the *d*-spacing of the collected solid (e.g. P-Mg_2FeCl-LDH) was similar to that of the pristine LDH (Table 1), i.e. TPP does not really intercalate into the interlayer, but is adsorbed on the surface and the near-edge interlayer, as addressed in Section 3.4.

Unlike Mg_2FeCl-LDH, Ca_2FeCl-LDH exhibits different uptake behavior. As shown in Fig. 3(b), in the lower equilibrium concentration range (0–0.5 mg/L), the uptake amount of TPP was almost linearly increased with the equilibrium concentration. When the equilibrium concentration was over 0.5 mg/L, the amount was only slightly increased until 40 mg/L. The maximum practical amount (56.4 mg/g) is very close to the theoretical maximum amount (60 mg/g) if assuming only the anion exchange is involved (assuming 0.64 mmol of TPP substitutes 3.2 mmol of Cl anions in 1 g of Ca_2FeCl-LDH). However, this is obviously not true as the collected solid is amorphous, not LDH phase. This removal is assumed to largely contribute to the dissolved Ca ions.

To estimate the contribution of dissolved Ca ions, the TPP adsorption was performed on HCa_2FeCl-LDH. As shown in Fig. 3(b), the TPP adsorption over HCa_2FeCl-LDH gave the adsorption amount of about 7.0 mg/g. As indicated in Table 1 as well as in following Eqs. (1) and (2), about 30 wt% of Ca_2FeCl-LDH is dissolved, thus the contribution from the left framework (HCa_2FeCl-LDH, 70 wt%) is only corresponding to 9% of total uptake by Ca_2FeCl-LDH. On the other hand, the adsorption amount per unit surface area over HCa_2FeCl-LDH is about 0.032 mg/m^2 (Table 1), much lower than 0.157 and 3.53 mg/m^2 over Mg_2FeCl-LDH and Ca_2FeCl-LDH, respectively (Table 2). This observation, together with the amorphous phase of P-Ca_2FeCl-LDH, suggests that the major removal of TPP over Ca_2FeCl-LDH is not dependent on the solid Fe-rich framework, but dependent on Ca^{2+} released from the LDH. The isotherm of Ca_2FeCl-LDH is so much different from those of MgFeCl-LDH and HCa_2FeCl-LDH that their removal mechanism should be fundamentally different. It is our belief that Ca_2FeCl-LDH is partially dissolved, releasing Ca^{2+} in a certain concentration. The released Ca^{2+} react

with TPP to form amorphous Ca-TPP precipitate, as reported elsewhere [29]. However, TPP is mainly taken up by Mg_2FeCl-LDH through exchanging the surface and near-edge Cl^-. More particularly, TPP is just adsorbed on the surface of HCa_2FeCl-LDH via relatively weak van der Waal's interactions.

3.3. Effects of TPP hydrolysis and the electrolyte

Hydrolysis of TPP to orthophosphate in aqueous solution may impact the TPP removal. As shown in Fig. 3(a), 0.3–0.5 mg/L of P in orthophosphate (ortho-P) was observed, indicating hydrolysis of TPP to ortho-P in both cases. The slight decrease of ortho-P from 0.4 to 0.2 mg/L within 8 h indicates formation of Ca-phosphate over LDHs [5]. Therefore, the ratio of ortho-P to total phosphate removed can be estimated by the reduction of ortho-P within 8 h. For Ca_2FeCl-LDH, Ca-phosphate (apatite) was about 2% of removed phosphates, which is probably amorphous as its XRD pattern was not detected.

However, the hydrolysis of TPP was very much limited in our experiments. For instance, in the case of Ca_2FeCl-LDH, after 24 h treatment, there was 78% of TPP remaining in the solution. The ortho-P percentage in total phosphate in the solution was only about 1.0% (0.35 mg/L/35 mg/L × 100%) (Fig. 3(a) and (b)). For Mg_2FeCl-LDH, the conversion percentage was about 1.2% based on the left TPP (96%).

Some reports showed that pH and the temperature play an important role in the hydrolysis of TPP. Zinder found at 40 °C and pH = 7, the hydrolysis rate constant was $4.81 \times 10^{-4}\ h^{-1}$ [11]. Only 1% of TPP conversion was observed at pH = 9 and 65 °C, and 19% conversion at 86 °C, after 22 h hydrolysis [24]. Therefore, the slow hydrolysis of TPP in the current cases is contributed to the higher pH (pH = 10) and lower temperature (25 °C).

In addition, the removal of TPP under the electrolyte background was investigated. As shown in Fig. 6, the removal amount of TPP over both LDHs in 0.1 M NaCl solution is similar to that in solution without the extra electrolyte. This indicates that the ionic strength has little effect on the removal of TPP. Over Mg_2FeCl-LDH, this is because of the stronger affinity of TPP for LDH as more negative charges of TPP than Cl^- [25]. In the case of Ca_2FeCl-LDH, precipitation of Ca-TPP seems not to be impacted by the ionic strength change.

3.4. Removal mechanism over LDHs

It is well understood that the anion uptake over MgAl-LDH is an anion exchange process. In general, the anion is first adsorbed on the external surface and edge, and then exchanges with the interlayer one [26,27]. This process is also reported to take place in phosphate adsorption over MgAl-LDH and MgFe-LDH. It is our belief that TPP adsorption over Mg_2FeCl-LDH follows the similar mechanism.

The XRD pattern of TPP-uptake Mg_2FeCl-LDH (P-Mg_2FeCl-LDH in Fig. 1(a)) still identifies the LDH structure, while the presence of Mg, Fe, and P is confirmed (Fig. 4(a) and (d)). However, the measured *d*-spacing was kept at 0.798 nm, not expanded to 0.95–1.0 nm for TPP intercalated LDH [25]. This indicates that TPP is mainly adsorbed on the external surface. We can also reasonably assume that some TPP is intercalated to the near-edge interlayer based on: (1) this intercalation interferes the LDH layer stacking and reduces the crystallites thickness (from 19.1 to 14.7 nm, Table 1); (2) the exposed surface can only adsorb about 5% of the theoretical amount of TPP as the LDH thickness of plane (0 0 3) is about 15–19 nm while the practical adsorption was 16% (10.5 vs. 67 mg/L). FTIR spectra confirmed the remaining LDH structure of P-Mg_2FeCl-LDH by the similar bands observed in Mg_2Fe-Cl-LDH (Fig. 2(a)). Moreover, the bands from 800 to 1220 cm^{-1} not observed in Mg_2Fe-Cl-LDH are attributed to P-oxo-anion taken up. The peaks at 904, 981, 1045, and 1126 cm^{-1} correspond to vibrations of P–O–P, P_2O_7, terminal PO_4 (symmetric), and terminal PO_4 (asymmetric), respectively [28]. A weak band was observed at 1213 cm^{-1} and assigned to the bridging PO_2, which is specially attributed to $P_3O_{10}^{5-}$ [29], indicating $P_3O_{10}^{5-}$ is present in P-Mg_2FeCl-LDH. In addition, the dissolution of Mg_2FeCl-LDH was observed during TPP removal. As listed in Table 4, a gradual releasing of Mg and Fe was observed during the removal of TPP. After 24 h, 20% of Mg and 1.5% of Fe were released into solution, indicating the molar ratio of Mg/Fe was about 1.5, in consistence with the ratio of solid sample in Table 1. This demonstrates the relative aqueous stability of Mg_2FeCl-LDH.

Table 4
Metal cation percentage (% = $M_{solution}/M_{total} \times 100$) releasing from LDH as the function of time in TPP removal.

Sample	Time (h)			
	0.5	1	2	24
Mg_2FeCl-LDH				
Mg	4.9	7.3	11	20
Fe	0.5	1.0	1.0	1.5
Ca_2FeCl-LDH				
Ca	44	46	46	49
Fe	0.0	0.0	0.0	0.0

On the other hand, TPP removal over Ca_2FeCl-LDH is very much different although the surface area of P-Ca_2FeCl-LDH (83 m^2/g) is similar to that of P-Mg_2FeCl-LDH (91 m^2/g). Table 4 also lists the amount of Ca released within 0.5 h, up to 44% of total Ca, but no Fe released. This indicates Ca_2FeCl-LDH is dissolved quickly. After 24 h, near 50% of Ca was determined in solution. It is consistent with the Ca/Fe molar ratio of 1.0 in P-Ca_2FeCl-LDH listed in Table 1, demonstrating the relatively instability of Ca_2FeCl-LDH in solution.

Apart from the much higher removal amount (56.4 mg/g) and the much slower removal rate, the collected TPP-uptake solid (P-Ca_2FeCl-LDH) is nearly amorphous (Fig. 1(b)). As shown in Fig. 2(b), the FTIR spectrum of P-Ca_2FeCl-LDH is much different from that of Ca_2FeCl-LDH and HCa_2FeCl-LDH. The bands of TPP were also observed in 800–1220 cm^{-1}, such as the strong vibration of P–O–P at 912 cm^{-1}, and the strong and broad band in 1000–1100 cm^{-1}, consisting overlapped asymmetric (1099 cm^{-1}) and symmetric (1035 cm^{-1}) vibrations of terminal PO_3. The band broadening is likely attributed to the effect of strong hydrogen bonds of water, as in $Ca_5(P_3O_{10})_2 \cdot nH_2O$ [20]. In addition, the band of CO_3 is weaker than that in H-Ca_2FeCl-LDH. Taking into account the weak peak of $CaCO_3$ in XRD pattern (Fig. 1(b)), the smaller amount of $CaCO_3$ formed is due to the inhibition of TPP to $CaCO_3$ precipitation since 78% TPP is still remained in solution after removal.

To know more about the structure and composition information, XPS analysis was conducted to characterize the amorphous compound (P-Ca_2FeCl-LDH), the hydrolyzed (HCa_2FeCl-LDH) and the pristine LDH (Ca_2FeCl-LDH), as presented in Fig. 5. The components of Fe 2p doublet (Fe $2p_{3/2}$ and Fe $2p_{1/2}$) are located at 711.3 and 724.9 eV in all three cases (Fig. 5(a)), revealing that Fe^{3+} is the main oxidation state in these solids existing in the form of $Fe(OH)_3$ and/or FeO(OH). This is reflected in the XPS at the O 1s core level (Fig. 5(b)). The deconvolution of the O 1s peak results in three peaks with the Gaussian shape, corresponding to O^{2-}, OH^- and H_2O, respectively, and their relative percentage in three solids is summarized in Table 5. Obviously, the predominant oxygen in Ca_2FeCl-LDH was OH^- (72.7%), and some was changed to O^{2-} (17.0%). After hydrolysis in water (HCa_2FeCl-LDH), the percentage of OH^- was decreased to 41.1% while that of O^{2-} increased to 47.8%, with the O^{2-}/OH^- molar

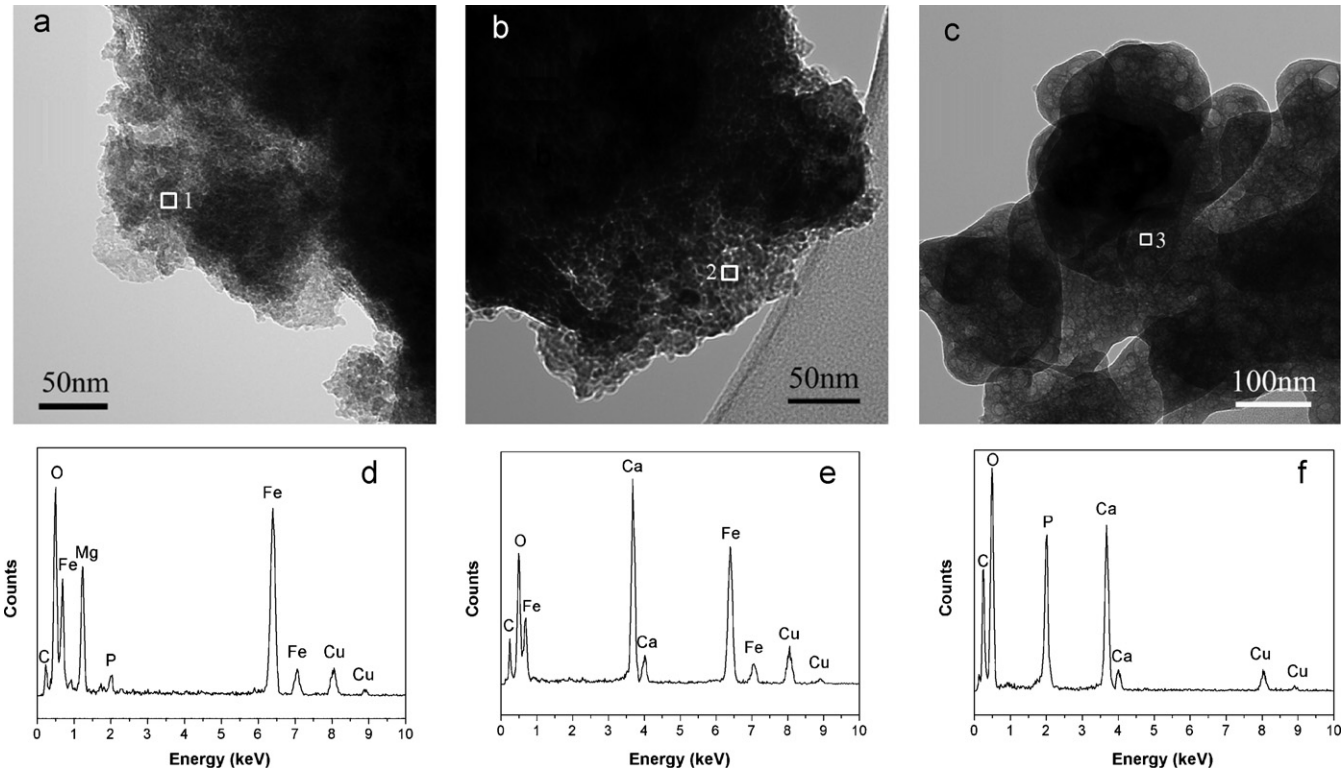

Fig. 4. TEM images of P-Mg_2FeCl-LDH (a) and P-Ca_2FeCl-LDH (b and c) with EDX spectra of region 1 (d), region 2 (e) and region 3 (f).

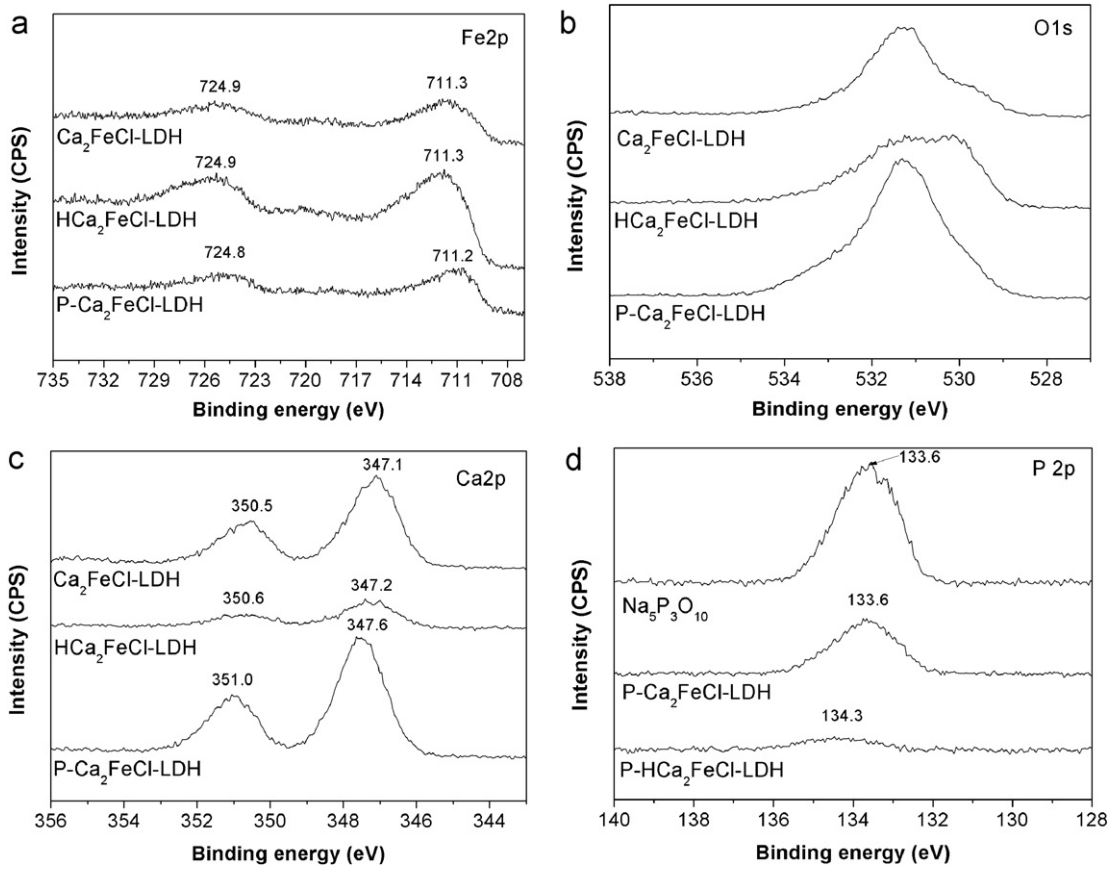

Fig. 5. Chemical shifts of Fe (a), O (b), Ca (c) and P (d) in the TPP removal on Ca_2FeCl-LDH and its hydrolyzed product.

Table 5
O 1s peak deconvolution of Ca_2FeCl-LDH before and after P removal and HCa_2FeCl-LDH.

Samples	Species[a]	Binding energy (eV)[b]	Percent (%)[c]
Ca_2FeCl-LDH	O^{2-}	529.8	17.0
	OH^-	531.3	72.6
	H_2O	532.9	10.3
HCa_2FeCl-LDH	O^{2-}	530.2	47.8
	OH^-	531.6	41.1
	H_2O	533.1	11.1
P-Ca_2FeCl-LDH	O^{2-}	530.1	16.0
	OH^-	531.3	67.4
	H_2O	533.0	16.6

[a] O^{2-}: oxygen bonded to metal; OH^-: hydroxyl bonded to metal; H_2O: surface and/or interlayer water.
[b] Fixed 1.6 eV as FWHM for each O peak.
[c] Percentage of the atomic concentration of each species to the total oxygen atoms.

ratio close to 1:1. Taking into account the leaching of Ca from LDH framework, we thus proposed the following hydrolysis:

$$Ca_2Fe(OH)_6Cl{\cdot}2H_2O \rightarrow Ca^{2+} + Ca_aFeO_{1-b}(OH)_{2a+2b}{\cdot}xH_2O + OH^- + H_2O \quad (1)$$

where a is small (0.24 in Table 1). The residual Ca has the BE similar to that in $Ca_2Fe(OH)_6Cl{\cdot}2H_2O$ (Fig. 5(c)), as expected.

In the case of P-Ca_2FeCl-LDH, the ratio of O^{2-} to OH^- was found similar to that in Ca_2FeCl-LDH. This means that there are much more OH^- groups in P-Ca_2FeCl-LDH than that in HCa_2FeCl-LDH (Table 5). This demonstrates that Eq. (1) occurs to a less extent in TPP solution than in TPP free solution, which is directly reflected by the bigger Ca/Fe ratio (1.04 vs. 0.24, Table 1). The less dissolution is also supported by the fact that the smaller pH (10.5) results from the Ca leaching during TPP uptake than that (11.2) in the TPP free solution (Table 2). Therefore, the Ca/P molar ratio in P-Ca_2FeCl-LDH can be estimated as 1.9, close to 2.0 determined in our elemental analysis. Considering the O^{2-}/OH^- molar ratio (1:4.2 from Table 5), the following reaction is proposed for the TPP removal, irrespective of the dissolution (Eq. (1)):

$$Ca_2Fe(OH)_6Cl{\cdot}2H_2O + P_3O_{10}{}^{5-} \rightarrow Ca_{1.04}FeO_{0.64}(OH)_{2.8}(P_3O_{10}{}^{5-})_{0.2}{\cdot}xH_2O \quad (2)$$

Note that the BE of Ca was shifted up by 0.4–0.5 eV (Fig. 5(c)), i.e. the chemical environment of Ca is somewhat different from that in $Ca_2Fe(OH)_6Cl{\cdot}2H_2O$. This shift could be attributed to Ca-phosphate bond [30], supposedly due to the formation of Ca^{2+}-TPP amorphous precipitate.

In addition, the BE peak of P 2p (Fig. 5(d)) was observed at 133.6 eV in P-Ca_2FeCl-LDH (the same as in $Na_5P_3O_{10}$) while 134.6 eV in P-HCa_2FeCl-LDH. The peak around 133.6 eV could be assigned to P_3O_{10} while 134.6 eV to PO_4 [30]. The only PO_4 peak in P-HCa_2FeCl-LDH implies the more hydrolysis of P_3O_{10} into PO_4.

Fig. 4(b) shows TEM image of the scale-work structure in P-Ca_2FeCl-LDH. EDX peaks due to Ca and Fe (Fig. 4(e)) illustrates the Fe-rich framework retaining some Ca. Very interestingly, the EDX peaks of amorphous precipitate only confirm the presence of Ca and P (Fig. 4(f)), indicating formation of Ca-TPP precipitate, without Fe in the structure. The formula of Ca-TPP precipitate was found to depend on the initial molar ratio of Ca/P in the solution [31]. In the initial $[Ca^{2+}]/[P] = 2.0–4.0$, $Ca_5(P_3O_{10})_2{\cdot}nH_2O$ was the dominative component [20]. In the current case, the initial $[Ca^{2+}]/[P]$ was estimated at about 2.6 if all Ca were leached out from LDH. Therefore, nominal formula $Ca_{1.04}FeO_{0.64}(OH)_{2.8}(P_3O_{10}{}^{5-})_{0.2}{\cdot}xH_2O$ in Eq. (2) consists of two compounds: $Ca_{0.54}FeO_{0.64}(OH)_{2.8}{\cdot}mH_2O$ and $Ca_{0.5}(P_3O_{10}{}^{5-})_{0.2}{\cdot}nH_2O$.

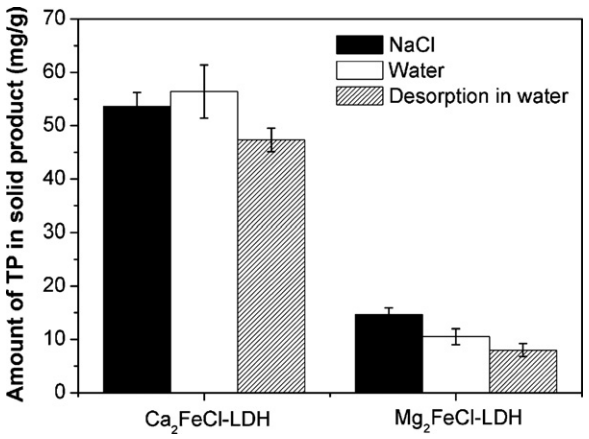

Fig. 6. Effect of ionic strength on the removal of TPP and reversibility of TPP loading products in water.

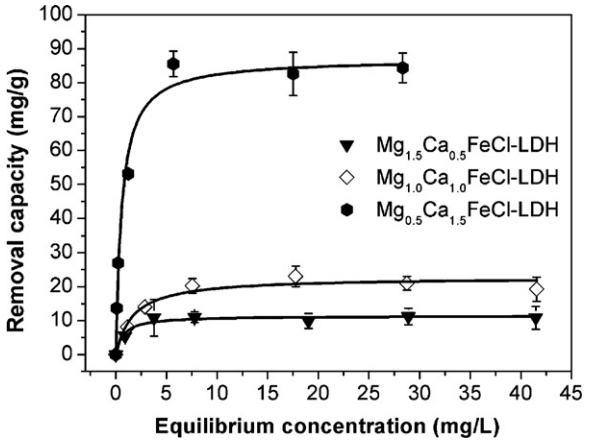

Fig. 7. Isotherm process of TPP over MgCaFe-LDHs. Solid lines refer to the removal trend on substrates.

The reversibility of products is shown in Fig. 6. After 24 h, about 80% P was retained in the precipitate in both cases of LDHs. This reveals the stability of P adsorbed samples. P releasing from P-uptake samples is likely contributed to dissolution of MgFe-P-LDH or $Ca_{0.5}(P_3O_{10}{}^{5-})_{0.2}{\cdot}nH_2O$.

3.5. Synergic TPP uptake by MgCaFe-LDH

As discussed above, Ca-LDH exhibited a higher removal amount of TPP than Mg-LDH via a different mechanism. In this connection, MgCaFe-LDH was prepared for the capture of TPP, in which the combination of both mechanisms is expected to probably improve the removal of TPP via synergic effect.

Fig. 7 shows the isotherm of TPP capture by MgCaFe-LDH as function of various Mg/Ca ratios. All of the experimental isotherms display the removal amount of TPP increased with the TPP equilibrium concentration and the experimental maximum uptake amount is summarized in Table 2. Like that over Mg_2Fe-Cl-LDH, the saturation uptake amount of TPP over $Mg_{1.5}Ca_{0.5}Fe$-Cl-LDH (10.7 mg/L) is only 17% of the theoretic one (61 mg/L), so the external surface adsorption is dominative. As expected, the increasing uptake amount of TPP is obtained over $Mg_{1.0}Ca_{1.0}Fe$-Cl-LDH and $Mg_{0.5}Ca_{1.5}Fe$-Cl-LDH. This demonstrates the dissolution-precipitation of Ca is a main mechanism to remove TPP. Especially over $Mg_{0.5}Ca_{1.5}Fe$-Cl-LDH, the saturation uptake amount of TPP (84.2 mg/L) is even higher than that over Ca_2Fe-Cl-LDH (56.4 mg/L).

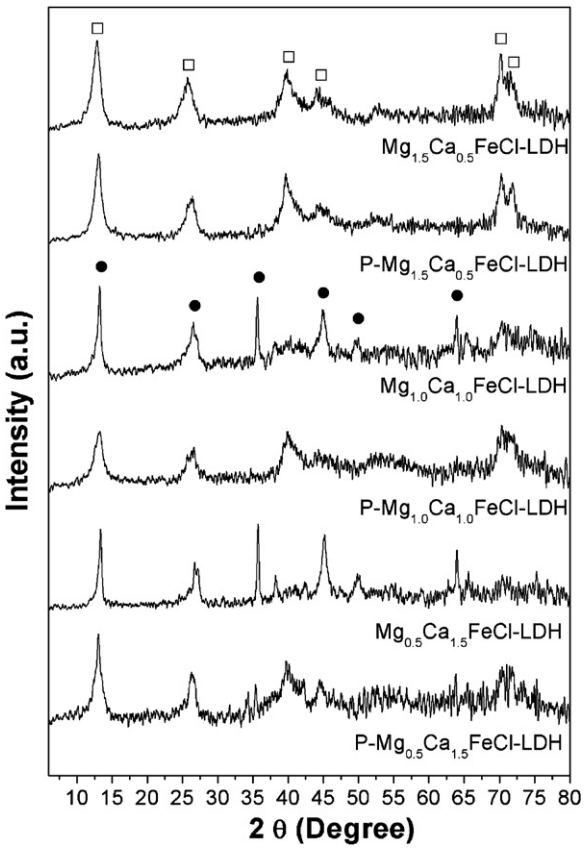

Fig. 8. XRD patterns of the LDHs and P loading products. Mg_2FeCl-LDH marked with square and Ca_2FeCl-LDH with circle.

Fig. 8 illustrates the XRD patterns of LDHs and their TPP-uptake solids. The typical characteristic diffractions of LDH structure were observed for the absorbents. However, the features of the Ca_2Fe-Cl-LDH structure were only observed in $Mg_{1.0}Ca_{1.0}Fe$-Cl-LDH and $Mg_{0.5}Ca_{1.5}Fe$-Cl-LDH, as reflected by marked peaks. Surprisingly, the layered structure was retained in all three cases. It seems that when the Mg/Fe ratio is not high enough to maintain the LDH structure, more Ca is retained in the LDH structure. This is supported by the factor that solution pH becomes less (9.3) when Mg/Ca is decreased (Table 2). Taking into account the high removal amount of TPP over $Mg_{0.5}Ca_{1.5}Fe$-Cl-LDH, we believe that the retaining of Ca in the LDH structure has positive effect on the improvement of TPP removal.

4. Conclusions

In the current work, TPP removal by MgCaFe-LDH was investigated. The removal isotherms indicate that TPP is removed on MgFe-Cl-LDH mainly by surface adsorption and near-edge intercalation, giving rise to the adsorption amount only 10.5 mg/g. On the contrary, the removal process of TPP by CaFe-Cl-LDH involves LDH-dissolution and precipitation as Ca-TPP compound, leading to the removal amount to 56.4 mg/g. Moreover, our research reveals that MgCaFe-LDH can remove TPP more efficiently. The removal process involves the adsorption/intercalation in MgCaFe-LDH structure and Ca-TPP precipitation, which enables $Mg_{0.5}Ca_{1.5}Fe$-Cl-LDH to capture 84.2 mg/g, a promising material for TPP removal.

Acknowledgments

This project is financially supported by National Nature Science Foundation of China No. 20677037, No. 20877053, National Major Science and Technology Program for Water Pollution Control and Treatment 2009ZX07106-01, 2008ZX0742-002 and Shanghai Leading Academic Discipline Project No. S30109. Dr. Xu acknowledges the financial support from the Australian Research Council for the ARC Centre of Excellence for Functional Nanomaterials and ARC Discovery project (DP0870769). This work is also supported by the State Scholarship Fund (No. 2009689027) by China Scholarship Council and Shanghai University Innovative Foundation for High Degree Student. We specially appreciate Mr. Yi Jia and Ms. Zi Gu for TEM/EDX and UV-spectrum determination, respectively.

References

[1] A.I. Khan, D. O'Hare, Intercalation chemistry of layered double hydroxides: recent developments and applications, J. Mater. Chem. 12 (2002) 3191–3198.
[2] K.H. Goh, T.T. Lim, Z. Dong, Application of layered double hydroxides for removal of oxyanions: a review, Water Res. 42 (2008) 1343–1368.
[3] J.Z. Zhou, G.R. Qian, Y.L. Cao, P.C. Chui, Y.F. Xu, Q. Liu, Transition of Friedel phase to chromate-AFm phase, Adv. Cement Res. 20 (2008) 167–173.
[4] Y.Y. Wu, Y. Chi, H.M. Bai, G.R. Qian, Y.L. Cao, J.Z. Zhou, Y.F. Xu, Q. Lu, Z.P. Xu, S.Z. Qiao, Effective removal of selenate from aqueous solutions by the Friedel phase, J. Hazard. Mater. 176 (2010) 193–198.
[5] Y.F. Xu, Y.C. Dai, J.Z. Zhou, Z.P. Xu, G.R. Qian, G.Q.M. Lu, Removal efficiency of arsenate and phosphate from aqueous solution using layered double hydroxide materials: intercalation vs. precipitation, J. Mater. Chem. 20 (2010) 4684–4691.
[6] Z.P. Xu, Y.G. Jin, S.M. Liu, Z.P. Hao, G.Q. Lu, Surface charging of layered double hydroxides during dynamic interactions of anions at the interfaces, J. Colloid Interface Sci. 326 (2008) 522–529.
[7] S.L. Chen, Z.P. Xu, Q. Zhang, G.Q.M. Lu, Z.P. Hao, S.M. Liu, Studies on adsorption of phenol and 4-nitrophenol on MgAl-mixed oxide derived from MgAl-layered double hydroxide, Sep. Purif. Technol. 67 (2009) 194–200.
[8] H.C. Greenwell, W. Jones, S.L. Rugen-Hankey, P.J. Holliman, R.L. Thompson, Efficient synthesis of ordered organo-layered double hydroxides, Green Chem. 12 (2010) 688–695.
[9] K. Xing, H.Z. Wang, L.G. Guo, W.D. Song, Z.P. Zhao, Adsorption of tripolyphosphate from aqueous solution by Mg–Al–CO_3-layered double hydroxides, Colloid Surf. A 328 (2008) 15–20.
[10] D.J. Halliwell, I.D. McKelvie, B.T. Hart, R.H. Dunhill, Hydrolysis of triphosphate from detergents in a rural waste water system, Water Res. 35 (2001) 448–454.
[11] B. Zinder, J. Hertz, H.R. Oswald, Kinetic-studies on the hydrolysis of sodium tripolyphosphate in sterile solution, Water Res. 18 (1984) 509–512.
[12] K. Okada, K. Nishimuta, Y. Kameshima, A. Nakajima, Effect on uptake of heavy metal ions by phosphate grafting of allophane, J. Colloid Interface Sci. 286 (2005) 447–454.
[13] E.I. Unuabonah, B.I. Olu-Owolabi, A.N. Oladoja, A.E. Ofomaja, Z.L. Yang, Pb/Ca ion exchange on kaolinite clay modified with phosphates, J. Soil Sediments 10 (2010) 1103–1114.
[14] Y. Seida, Y. Nakano, Removal of phosphate by layered double hydroxides containing iron, Water Res. 36 (2002) 1306–1312.
[15] APHA, Standard Methods for the Examination of Water and Wastewater, 18th ed., American Public Health Association, Washington, DC, 1992.
[16] J. Zhang, Y.F. Xu, G.G. Qian, Z.P. Xu, C. Chen, Q. Liu, Reinvestigation of dehydration and dehydroxylation of hydrotalcite-like compounds through combined TG–DTA-MS analyses, J. Phys. Chem. C 114 (2010) 10768–10774.
[17] F. Millange, R.I. Walton, L.X. Lei, D. O'Hare, Efficient separation of terephthalate and phthalate anions by selective ion-exchange intercalation in the layered double hydroxide $Ca_2Al(OH)(6)$center dot NO_3 center dot 2H(2)O, Chem. Mater. 12 (2000) 1990–1994.
[18] S.J. Palmer, R.L. Frost, T. Nguyen, Hydrotalcites and their role in coordination of anions in Bayer liquors: anion binding in layered double hydroxides, Coord. Chem. Rev. 253 (2009) 250–267.
[19] R.L. Frost, H.J. Spratt, S.J. Palmer, Infrared and near-infrared spectroscopic study of synthetic hydrotalcites with variable divalent/trivalent cationic ratios, Spectrochim. Acta A 72 (2009) 984–988.
[20] Y. Zhou, J.O. Carnali, Solid-state hydrolysis of calcium tripolyphosphate scales, Langmuir 16 (2000) 5159–5168.
[21] D.R. Lide (Ed.), CRC Handbook of Chemistry and Physics, Boca Raton, FL, 2007.
[22] L. Lv, J. He, M. Wei, D.G. Evans, Z.L. Zhou, Treatment of high fluoride concentration water by MgAl–CO_3 layered double hydroxides: kinetic and equilibrium studies, Water Res. 41 (2007) 1534–1542.
[23] A. Ookubo, K. Ooi, H. Hayashi, Preparation and phosphate ion-exchange properties of a hydrotalcite-like compound, Langmuir 9 (1993) 1418–1422.
[24] J. Green, Reversion of molecularly dehydrated sodium phosphates, Ind. Eng. Chem. 42 (1950) 1542–1546.
[25] M. Badreddine, A. Legrouri, A. Barroug, A. De Roy, J.P. Besse, Ion exchange of different phosphate ions into the zinc–aluminium–chloride layered double hydroxide, Mater. Lett. 38 (1999) 391–395.
[26] T. Toraishi, S. Nagasaki, S. Tanaka, Adsorption behavior of IO^{3-} by CO_3^{2--} and NO^{3--} hydrotalcite, Appl. Clay Sci. 22 (2002) 17–23.
[27] S.L. Wang, C.H. Liu, M.K. Wang, Y.H. Chuang, P.N. Chiang, Arsenate adsorption by Mg/Al–NO_3 layered double hydroxides with varying the Mg/Al ratio, Appl. Clay Sci. 43 (2009) 79–85.

[28] X.H. Guan, Q. Liu, G.H. Chen, C. Shang, Surface complexation of condensed phosphate to aluminum hydroxide: an ATR-FTIR spectroscopic investigation, J. Colloid Interface Sci. 289 (2005) 319–327.
[29] W.Q. Gong, A real time in situ ATR-FTIR spectroscopic study of linear phosphate adsorption on titania surfaces, Int. J. Miner. Process. 63 (2001) 147–165.
[30] T.V. Vasudevan, P. Somasundaran, C.L. Howiemeyers, D.L. Elliot, K.P. Anan-thapadmanabhan, Interaction of pyrophosphate with calcium phosphates, Langmuir 10 (1994) 320–325.
[31] W.J. Diamond, J.E. Grove, Composition of the solid phase in the $Na_5P_3O_{10}$–$CaCl_2$–H_2O system, J. Phys. Chem. 63 (1959) 1528–1529.